Electronic Supplementary Material (ESI) for Nanoscale Advances.

ELECTRONIC SUPPLEMENTARY INFORMATION

CdS Crown Growth on CdSe Nanoplatelets: Core Shape Matters

Anja Schlosser,[a,b] *Rebecca T. Graf,*[a,b] *and Nadja C. Bigall*[*a,b,c]

[a] Institute of Physical Chemistry and Electrochemistry, Leibniz Universität Hannover, 30167 Hannover, Germany

[b] Laboratory of Nano and Quantum Engineering (LNQE), Leibniz Universität Hannover, 30167 Hannover, Germany

[c] Cluster of Excellence PhoenixD (Photonics, Optics, and Engineering Innovation Across Disciplines), Leibniz Universität Hannover, 30167 Hannover, Germany

* nadja.bigall@pci.uni-hannover.de

Contents

1 Characterisation of CdSe core nanoplatelets (NPLs). 2
1.1 Small quasi-rectangular 4 monolayer (ML) NPLs. 2
1.2 Large quasi-rectangular 4 ML NPLs. 3
1.3 Quasi-quadratic 4 ML NPLs. 4
1.4 Large quasi-rectangular 5 ML NPLs. 5

2 Details on the approximation of the CdS crown area. 6

3 Further results of syntheses with S/ODE as sulphur precursor. 8

4 Further characterisation results for CdSe/CdS core/crown NPLs with an increased crown thickness. 10

5 Results of powder X-ray diffractometry (PXRD). 15
5.1 4 ML CdSe/CdS core/crown NPLs with small quasi-quadratic cores. 15
5.2 4 ML CdSe/CdS core/crown NPLs with small quasi-rectangular cores. 16
5.3 4 ML CdSe/CdS core/crown NPLs with large quasi-rectangular cores. 17
5.4 5 ML CdSe/CdS core/crown NPLs with large quasi-rectangular cores. 18

6 TEM characterisation of 4 ML CdSe/CdS NPLs synthesised from small quasi-rectangular CdSe NPLs. 19

7 Further optical characterisation of CdSe/CdS NPLs synthesised from quasi-rectangular 4 and 5 ML CdSe NPLs. 20

8 Up-scaling of the synthesis procedure. 22

9 Comparison to CdSe and CdTe crown growth. 23

1 Characterisation of CdSe core nanoplatelets (NPLs).

1.1 Small quasi-rectangular 4 monolayer (ML) NPLs.

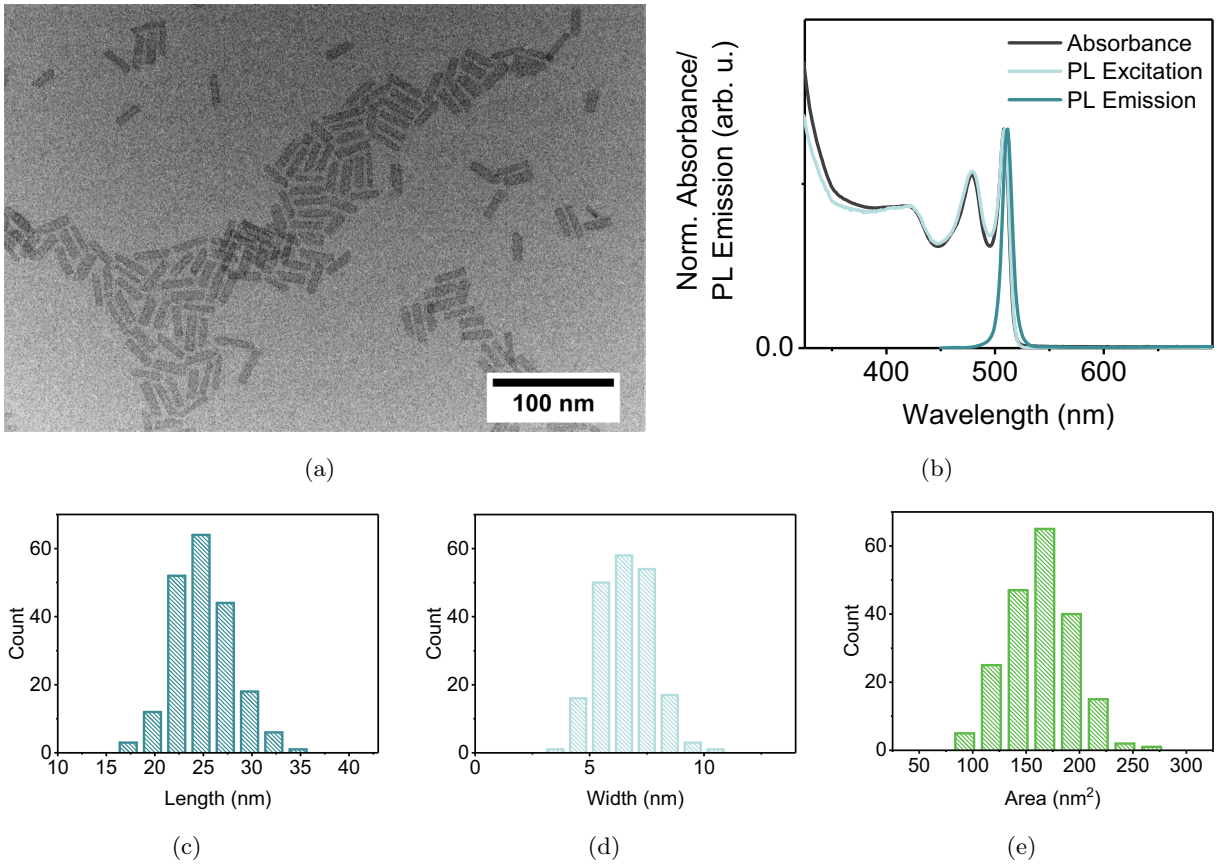

Figure S1. Characterisation results of small quasi-rectangular CdSe core NPLs with a thickness of 4 MLs. (a) In the overview TEM image the quasi-rectangular shape of the NPLs is visible. The corners of some NPLs appear to be slightly rounded. (b) Normalised absorbance (grey), photoluminescence (PL) excitation (light blue) and PL emission spectrum of a NPL solution. The absorbance maxima corresponding to the heavy hole-electron (hh-e) and the light hole-electron (lh-e) transition [1] are located at 508 nm and 479 nm, respectively. The PL excitation spectrum matches well with the absorbance spectrum, so nearly no other emitting or non-emitting species are present. The PL emission maximum is located at 511 nm. An absolute PL quantum yield (PLQY) of 8.0 % was determined for the purified NPL solution. (c)-(e) Distributions (n=200) of the NPL lengths (c), widths (d) and area (e). Mean values are: 24.9 nm ± 3.0 nm (length), 6.6 nm ± 1.2 nm (width) and 163.1 nm^2 ± 30.5 nm^2 (area).

1.2 Large quasi-rectangular 4 ML NPLs.

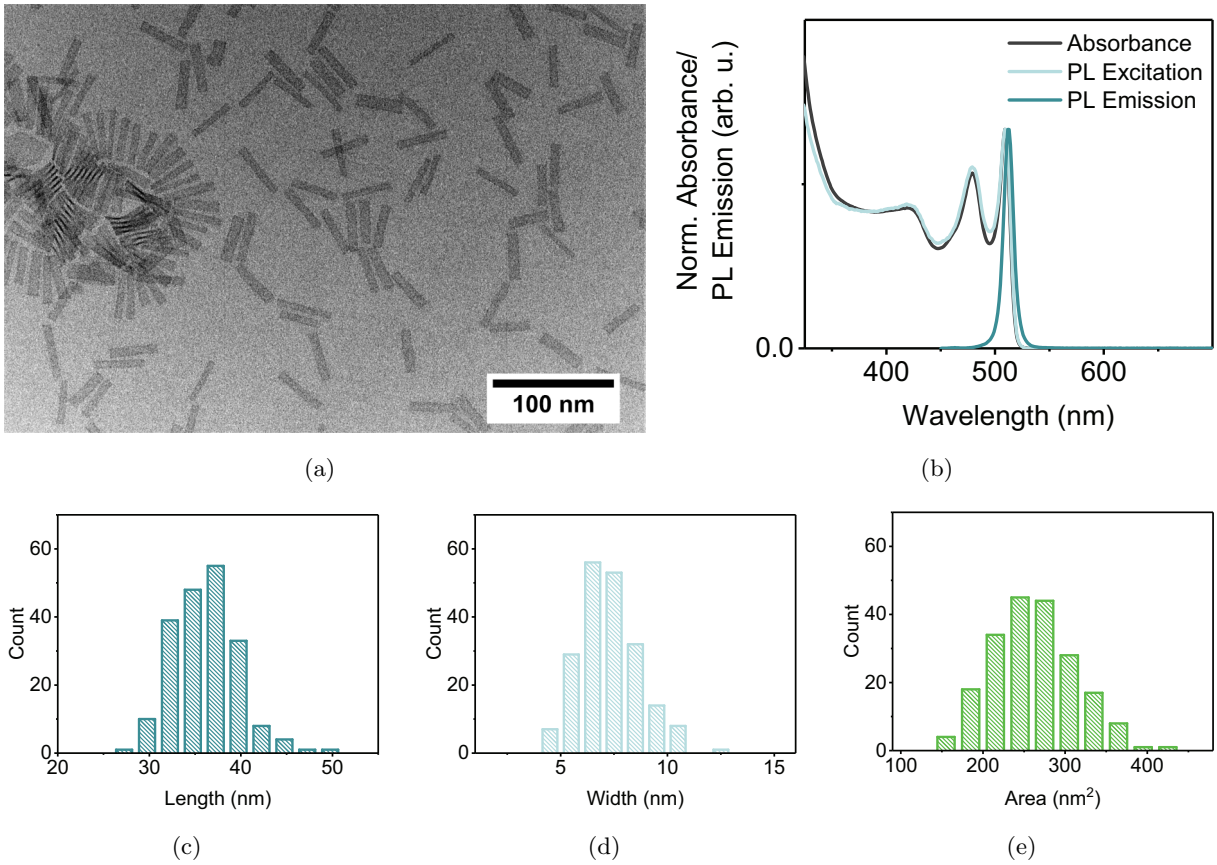

Figure S2. Characterisation results of large quasi-rectangular CdSe core NPLs with a thickness of 4 MLs. (a) The overview TEM image shows, that the quasi-rectangular shape of the NPLs was retained. Due to the extension, the aspect ratio (length/width) was observed to increase from 3.9 ± 1.0 (small quasi-rectangular NPLs) to 5.2 ± 1.2 and the corners of the NPLs appear to be sharper. (b) Normalised absorbance (grey), PL excitation (light blue) and PL emission spectrum of a solution of larger NPLs. The absorption maxima are located at 509 nm (hh-e transition) and 479 nm (lh-e transition). The PL emission maximum is located at 511 nm. An absolute PLQY of 51.0 % was determined for the large CdSe NPLs. (c)-(e) Distributions (n=200) of the NPL lengths (c), widths (d) and area (e). Mean values are: 36.1 nm ± 3.5 nm (length), 7.3 nm ± 1.4 nm (width) and 261.7 nm^2 ± 50.3 nm^2 (area).

1.3 Quasi-quadratic 4 ML NPLs.

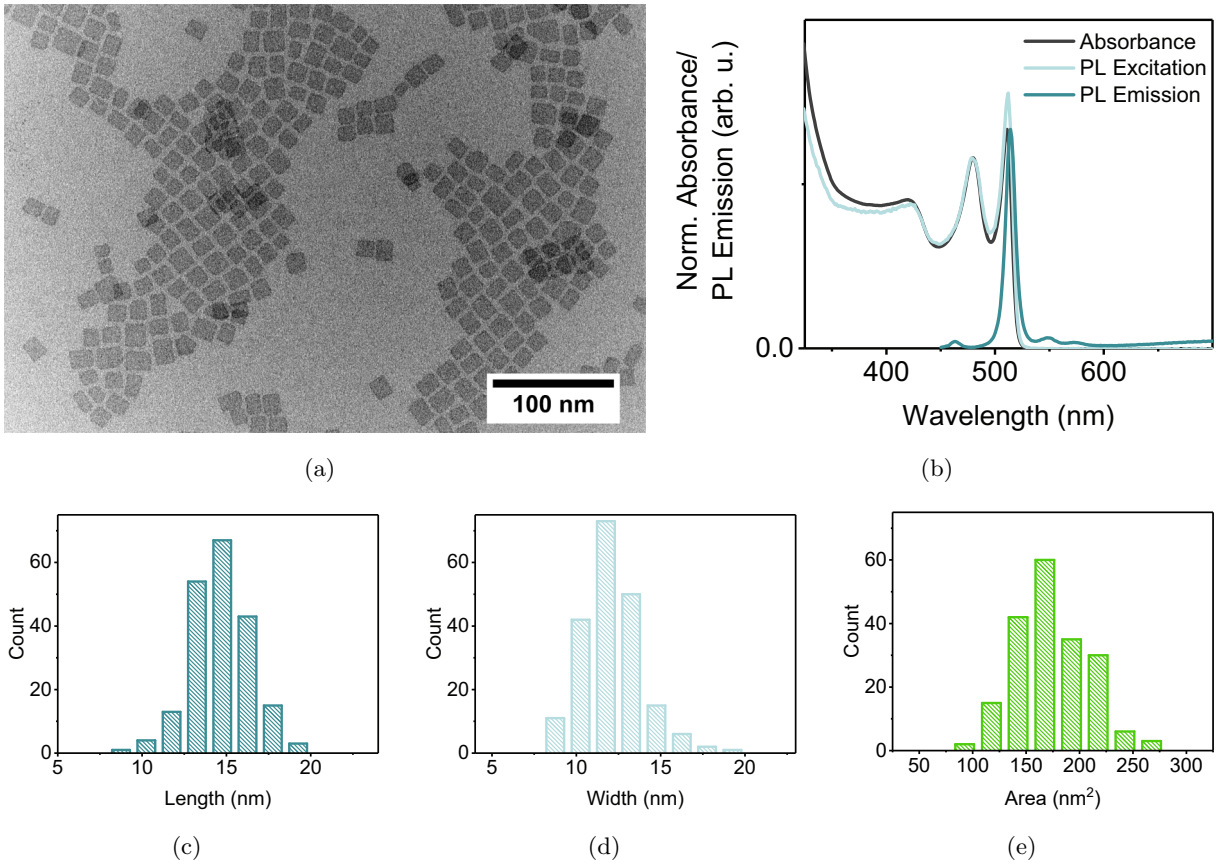

Figure S3. Characterisation results of large quasi-rectangular CdSe core NPLs with a thickness of 4 MLs. (a) In the overview TEM image the quasi-quadratic shape of the NPLs (aspect ratio: 1.2 ± 0.2) is visible. The corners of the NPLs are slightly rounded. (b) Normalised absorbance (grey), PL excitation (light blue) and PL emission spectrum of a solution of quasi-quadratic NPLs. The absorption maxima are located at 511 nm (hh-e transition) and 480 nm (lh-e transition). In the PL emission spectrum, some other emission peaks than the emission maximum corresponding to 4 ML NPLs (514 nm) are visible. However, as can be deduced from the PL extinction spectrum, the amount of impurities in total is negligible. The absolute PLQY was determined to be 0.7 % after the extensive purification. (c)-(e) Distributions (n=200) of the NPL lengths (c), widths (d) and area (e). Mean values are: 14.6 nm ± 1.8 nm (length), 12.1 nm ± 1.7 nm (width) and 178.0 nm^2 ± 41.9 nm^2 (area).

1.4 Large quasi-rectangular 5 ML NPLs.

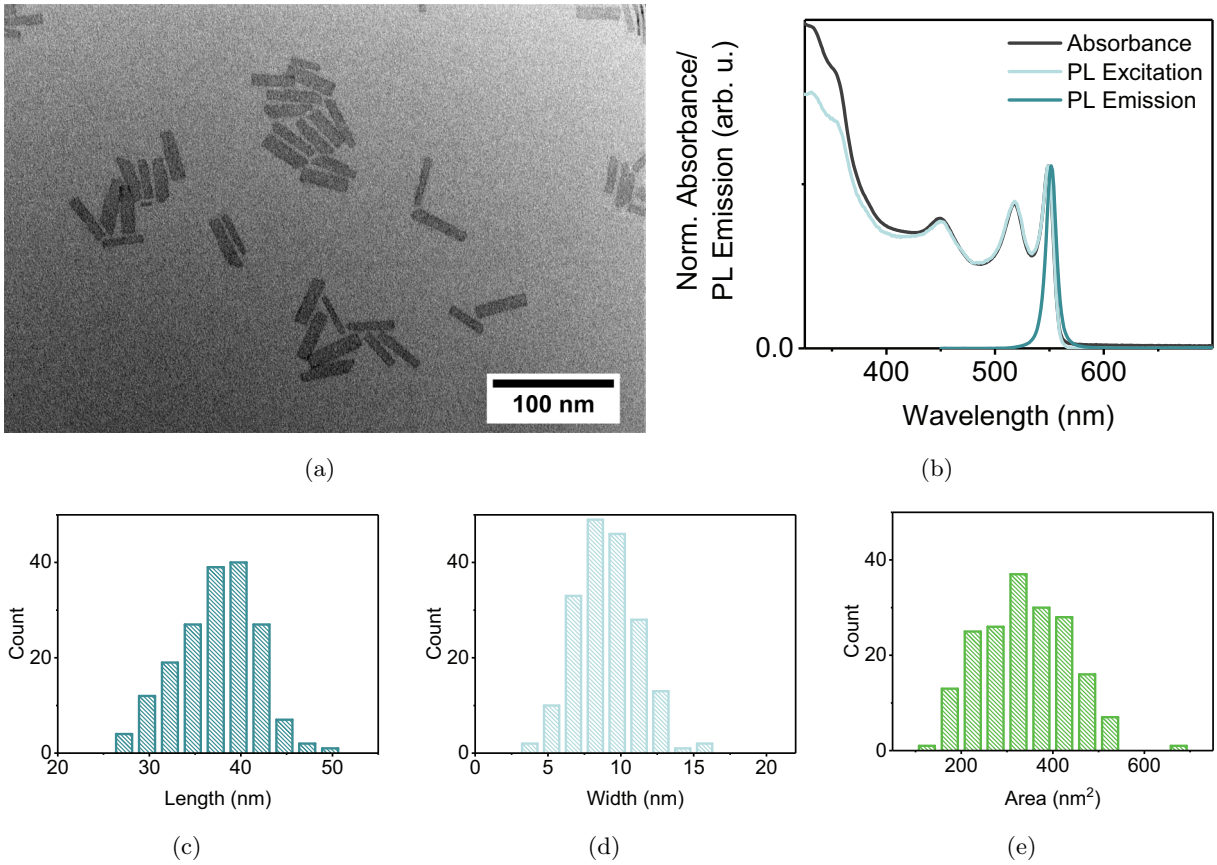

Figure S4. Characterisation results of large quasi-rectangular CdSe core NPLs with a thickness of 5 MLs. (a) The overview TEM illustrates the quasi-rectangular shape of the NPLs with slightly rounded and partly truncated corners. (b) Normalised absorbance (grey), photoluminescence (PL) excitation (light blue) and PL emission spectrum of a NPL solution. The absorption maxima are located at 549 nm (hh-e transition) and 518 nm (lh-e transition). The PL emission maximum is located at 552 nm. The absolute PLQY of the purified NPLs was determined to be 31.5 %. (c)-(e) Distributions (n=184) of the NPL lengths (c), widths (d) and area (e). Mean values are: 37.3 nm ± 5.0 nm (length), 9.0 nm ± 2.2 nm (width) and 338.6 nm^2 ± 96.8 nm^2 (area).

2 Details on the approximation of the CdS crown area.

To determine the area of the CdS crown solely from absorbance measurements, a relation between the specific absorption features of the NPLs and the NPL areas derived from TEM images needs to be established. Therefore, the NPL dimensions of in total 32 core/crown NPL samples, which were synthesised from different core NPLs, were measured. By including the dimensions of the core NPLs themselves, the CdS:CdSe area ratio $A_{\mathrm{CdS}}/A_{\mathrm{CdSe}}$ is obtained:

$$\frac{A_{\mathrm{CdS}}}{A_{\mathrm{CdSe}}}\ (n\ \mathrm{min}) = \frac{A_{\mathrm{total}}\ (n\ \mathrm{min}) - A_{\mathrm{core}}}{A_{\mathrm{core}}} \tag{1}$$

From the absorbance spectra, the y-values at the first (Abs 1) and third (Abs 3) absorbance maximum [Figure S5 (a)] are required. The ratio of both values can either be directly related to the area ratio [as in Figure 2 (c)] or it can be corrected with a core NPL specific factor [as in Figure S5 (b)]. This factor originates from the fact, that the Abs ratios of the different core NPLs depend on the NPL aspect ratio and thickness. The Abs ratio (as applied in the main text) and the corrected Abs ratio are calculated as follows:

$$\text{Abs ratio} = \frac{\text{Abs 3 } (n\ \mathrm{min})}{\text{Abs 1 } (n\ \mathrm{min})} \tag{2}$$

$$\text{Abs ratio (corrected)} = \frac{\text{Abs 3 } (n\ \mathrm{min})}{\text{Abs 1 } (n\ \mathrm{min})} - \frac{\text{Abs 3 } (0\ \mathrm{min})}{\text{Abs 1 } (0\ \mathrm{min})} \tag{3}$$

In Figure S5 (b), the area ratios were plotted against the corrected Abs ratios. By performing linear regressions on the different core NPL specific datasets, response factors can be obtained, which can later be used to compare the growth rates of CdSe/CdS core/crown NPLs synthesised from different core NPLs.

It needs to be noted, that the errors of high area and Abs ratios are generally larger than those of smaller ones. This is related to two factors: (1) large NPLs tend be either twisted or stacked if deposited onto TEM grids. Only the dimensions of flat-lying NPLs were determined, which might lead to rather large errors, as those NPLs might not be a representative image of the whole sample. (2) In some of the reactions, especially if no TOP was applied, some CdS NCs formed at the end of the reactions. Although all aliquots were cleaned by precipitation of the NPLs and subsequent centrifugation, a small amount of residual CdS NCs might remain in the samples later analysed by UV/Vis spectroscopy. This would lead to slightly higher absorbance values at the third absorbance maximum and therewith a higher Abs ratio.

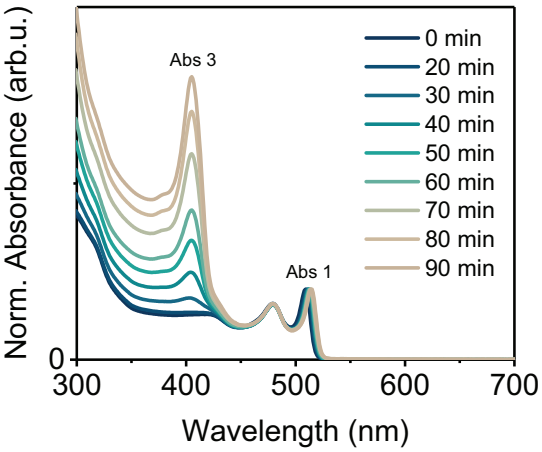

(a)

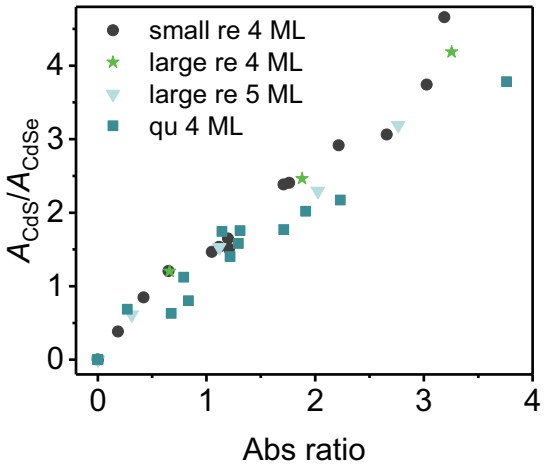

(b)

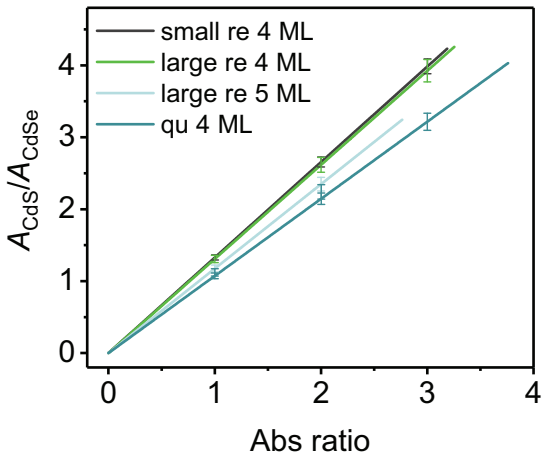

(c)

Figure S5. (a) Normalised absorbance spectra of CdSe/CdS core/crown NPLs with different crown sizes. For the calculation of the absorbance ratio (Abs ratio), the absorbance values at the first (Abs 1) and the third (Abs 3) absorbance maximum are required. (b) Ratio between the CdS and CdSe area (A_{CdS}/A_{CdSe}) of CdSe/CdS core/crown NPLs (derived from TEM images) plotted against the corrected Abs ratio. For the calculation of A_{CdS}/A_{CdSe}, the CdSe area was considered to be constant throughout the reaction. (c) Linear regressions obtained by fitting the data points shown in (c). The regression parameters are collected in Table S1.

Table S1. Regression parameters obtained from fits of the data points shown in Figure S5 (b)

core geometry	core thickness	slope	regression coefficient R^2
small quasi-rectangular	4 ML	1.328 ± 0.035	0.9898
large quasi-rectangular	4 ML	1.308 ± 0.052	0.9937
large quasi-rectangular	5 ML	1.174 ± 0.047	0.9920
small quasi-quadratic	4 ML	1.072 ± 0.040	0.9784

3 Further results of syntheses with S/ODE as sulphur precursor.

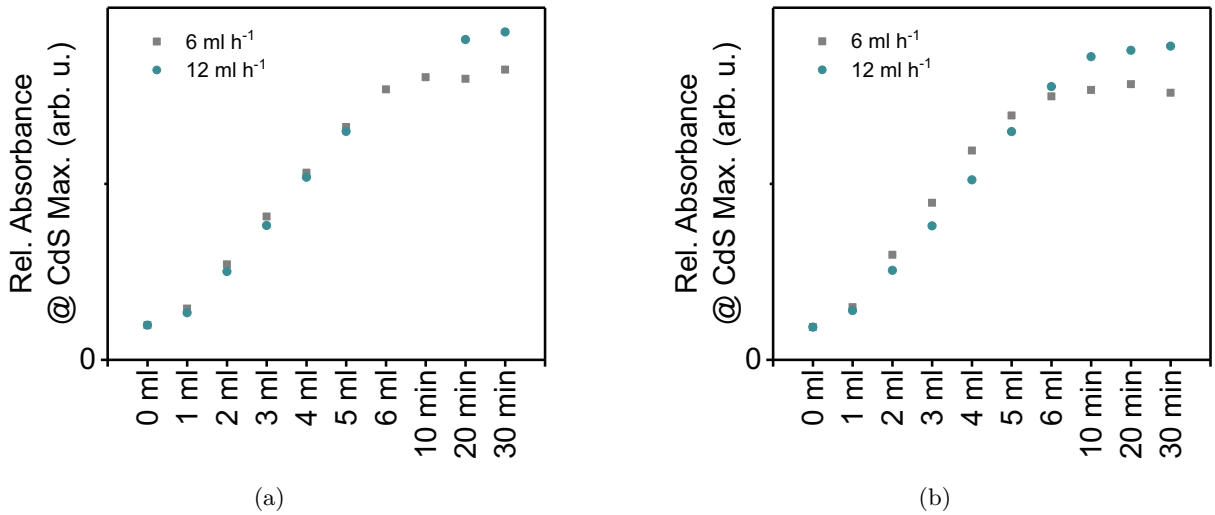

Figure S6. Progress of CdS crown growth at different precursor injection rates on (a) quasi-quadratic and (b) small quasi-rectangular 4 ML NPLs. In total, 6 mL of a S/ODE precursor solution were injected. The reaction duration (precursor injection + growth) was 90 min and 60 min for injection at 6 mL h^{-1} and 12 mL h^{-1}, respectively. Both y-axes are scaled similarly.

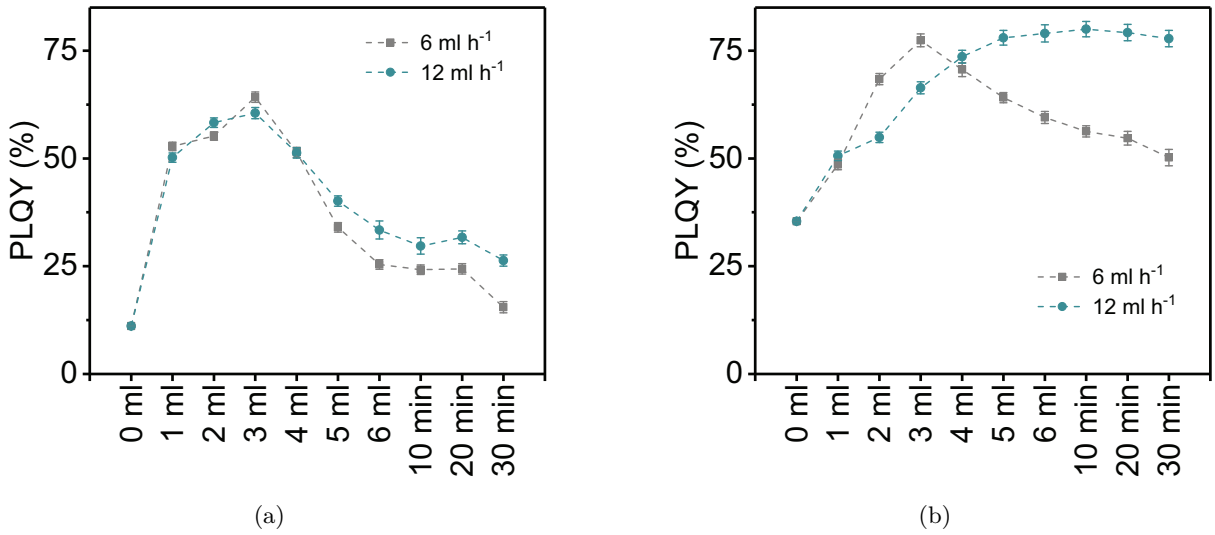

Figure S7. Development of PLQY (excitation wavelength: 460 nm) during the CdS crown growth reactions shown in Figure S6. (a) In case of quasi-quadratic core NPLs, a maximum PLQY is observed at a relatively small CdS crown size independent of the injection rate. (b) In case of quasi-rectangular core NPLs, different trends are observed. At an injection rate of 6 mL h^{-1}, the relation between PLQY and crown size is very similar to that for quasi-quadratic core NPLs. In contrast, if a higher injection rate is applied, the PLQY maximum is located at much higher crown sizes. This suggests, that at first a CdS crown with a comparably high defect density is formed, which is reduced later on.

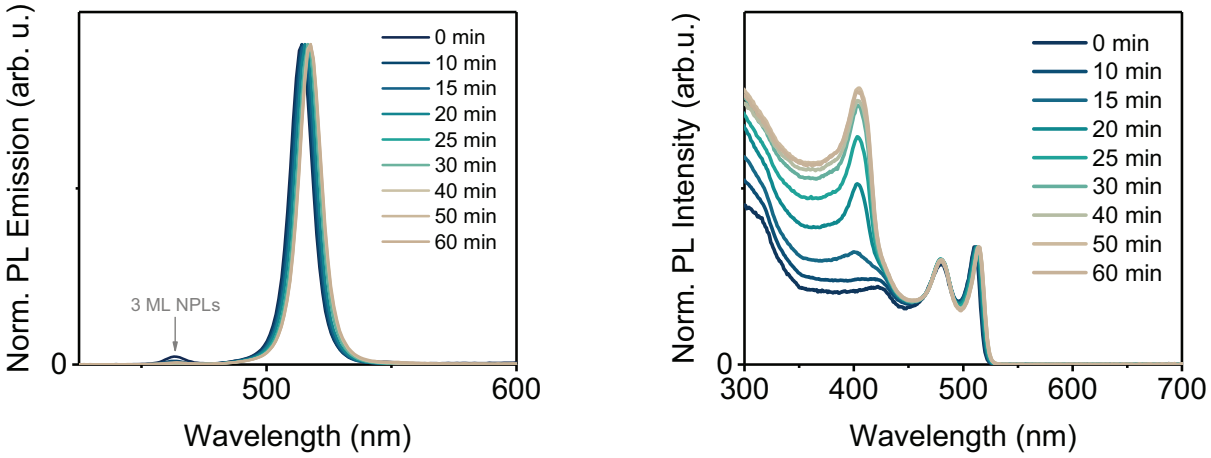

(a) (b)

Figure S8. (a) PL emission and (b) PL excitation spectra of CdSe/CdS NPLs synthesised from quasi-quadratic CdSe NPLs. Reaction conditions: 6 mL S/ODE, injection rate: 12 mL h^{-1}, 50 µL of TOP were added before the precursor injection. The PL excitation spectra were recorded at the emission maximum of the respective sample.

4 Further characterisation results for CdSe/CdS core/crown NPLs with an increased crown thickness.

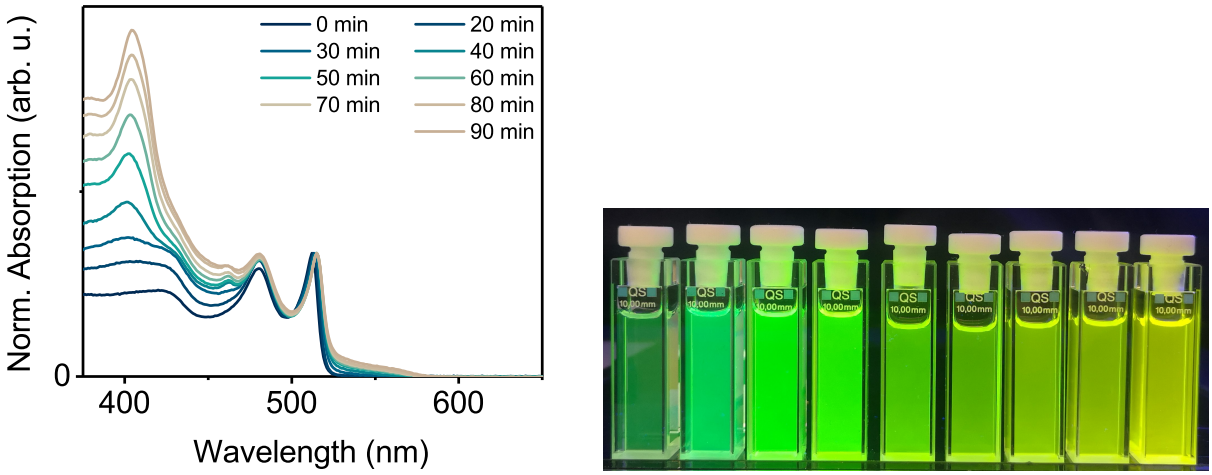

(a) (b)

Figure S9. (a) UV/Vis absorption spectra of CdSe/CdS NPLs synthesised from quasi-quadratic core NPLs at a rate of 6 mL h^{-1}. (b) Photograph of CdSe/CdS NPL solutions obtained with the mentioned reaction conditions under UV irradiation. The fluorescence colour changes over the course of the reaction (left cuvette: 0 min, right cuvette: 90 min) from green to yellow. The PLQY of samples showing only bathochromically shifted emission can reach up to 70 %.

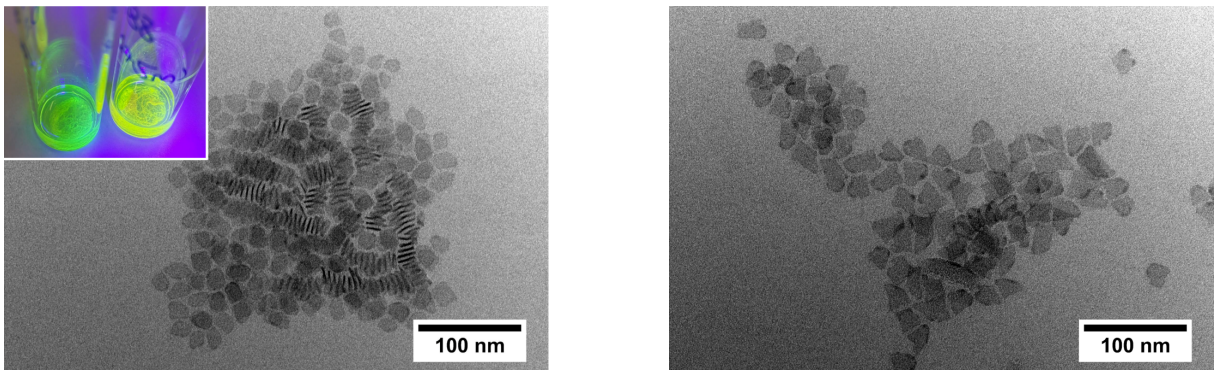

(a) (b)

Figure S10. Overview TEM images of CdSe/CdS NPLs synthesised from quasi-quadratic core NPLs at a rate of 6 mL h^{-1}. (a) after 30 min reaction time, (b) after 50 min reaction time. Especially at the early stages of the reaction, the NPLs tend to form stacks and even macroscopic filaments [inset in (a)], which can only partly be redissolved by ultrasonication.

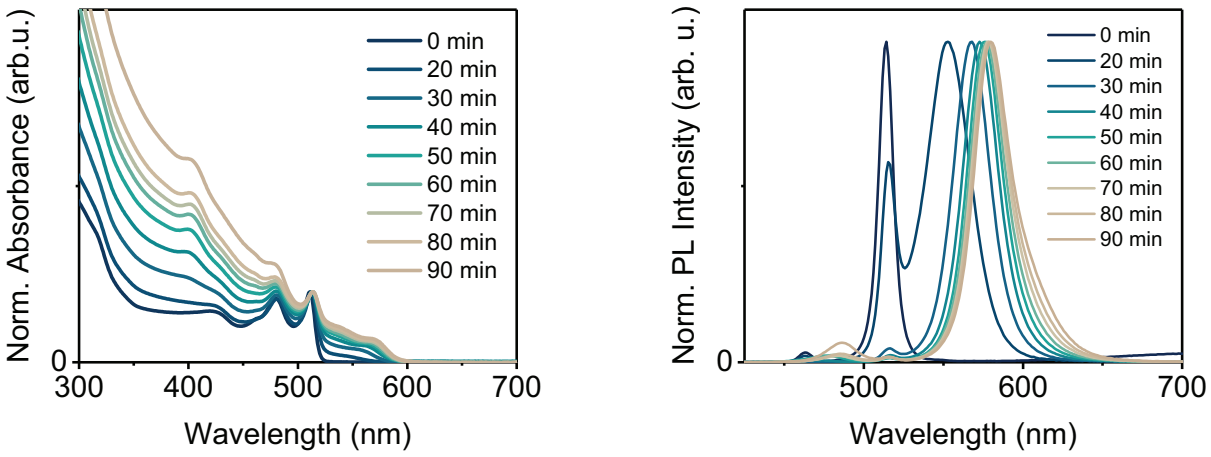

(a) (b)

Figure S11. (a) Normalised absorbance and (b) PL emission spectra of CdSe/CdS core/crown NPLs synthesised from quasi-quadratic core NPLs at a rate of 6 mL h^{-1} applying the double amounts of cadmium acetate dihydrate [$Cd(Ac)_2$] and oleic acid (OlA). All other reaction parameters were kept constant. Compared to the reaction with the single amount of $Cd(Ac)_2$ and OlAc, the formation of a thicker crown is visible at earlier reaction stages. At the end of the reaction, distinct absorption features are observed in the wavelength regime between 520 nm and 600 nm In the emission spectrum, an additional peak at around 480 nm appears due to the formation of spherical CdS NCs. Furthermore, the formation of a dark red precipitate, probably CdO, was observed.

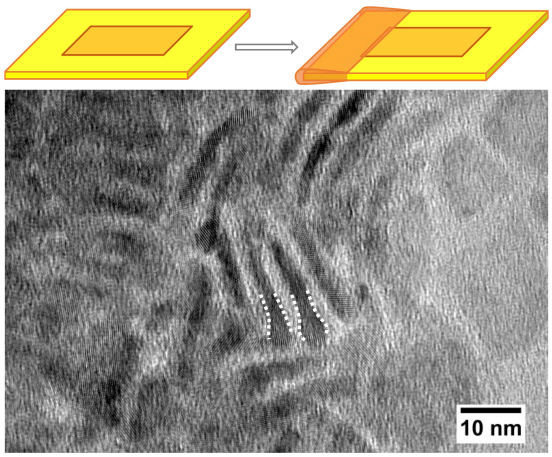

(a)

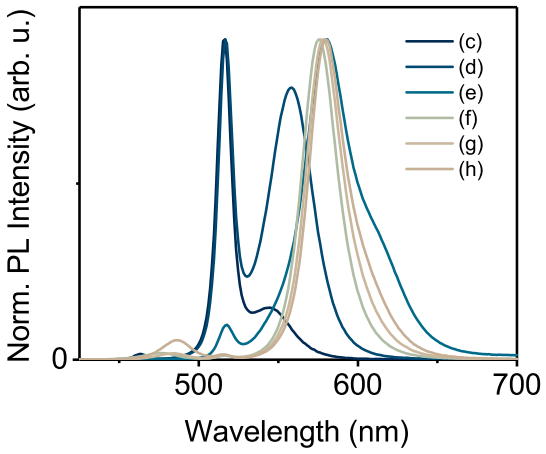

(b)

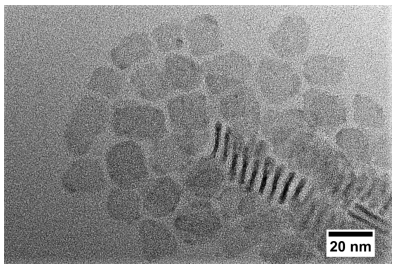

(c)

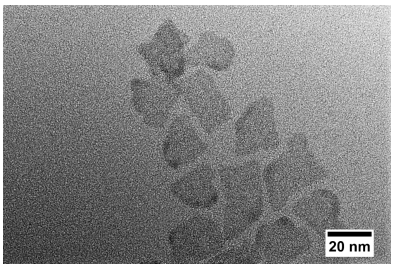

(d)

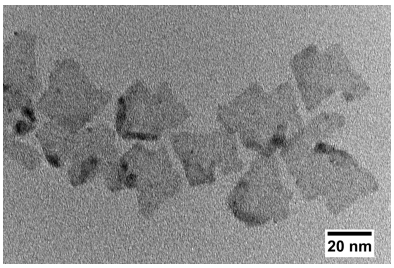

(e)

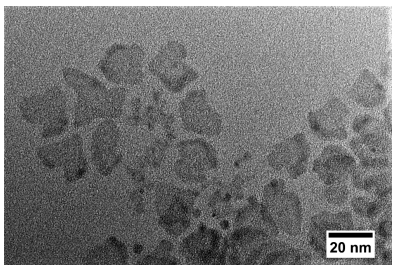

(f)

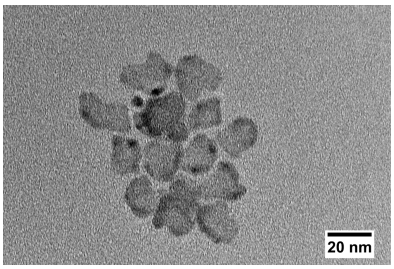

(g)

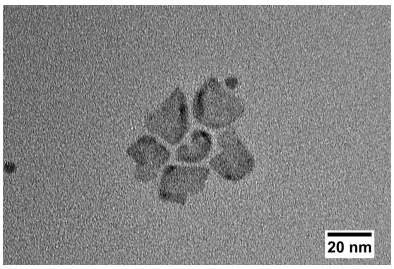

(h)

Figure S12. Morphological and spectroscopic characterisation of CdSe/CdS core/crown NPLs with an increased crown thickness at different reaction stages. (a) TEM image of stacked thick-crown NPLs. Due to the increased material thickness, NPLs standing perpendicular to the TEM grid appear as dark stripes. The NPL thickness is observed to increase continuously at one NPL edge, no distinct steps are visible. The white dotted lines were inserted to enhance the visibility of the NPL shape. (b) Emission spectra of the NPL samples shown in (c)-(h). (c)-(h) TEM images CdSe/CdS core/crown NPLs with an increased crown thickness at different reaction stages. (c)-(e) TEM images of CdSe/CdS NPLs synthesised with the single amounts of $Cd(Ac)_2$ and OlA at an injection rate of $6\,mL\,h^{-1}$. The samples were taken after (c) 30 min, (d) 50 min and (e) 150 min of total reaction time, respectively. (f)-(h) TEM images of CdSe/CdS NPLs synthesised with the double amounts of $Cd(Ac)_2$ and OlA at an injection rate of $6\,mL\,h^{-1}$. The samples were taken after (f) 50 min, (d) 70 min and (e) 90 min of total reaction time, respectively. Some spherical particles, probably homogeneously nucleated CdS, are visible. As can be seen in (c) and (d), the crown thickness starts to increase at the corners of the NPLs first (darker spots). (e)-(h) At later reaction stages or if a higher Cd precursor amount is applied, larger parts close to the NPL edges appear to be darker and therefore thicker. However, as can be seen especially in (e), (g) and (h), it is not possible to obtain a homogeneous ring around the NPL edge. We therefore conclude that 3D growth is favored only on some of the edges over 2D growth ("normal" crown growth).

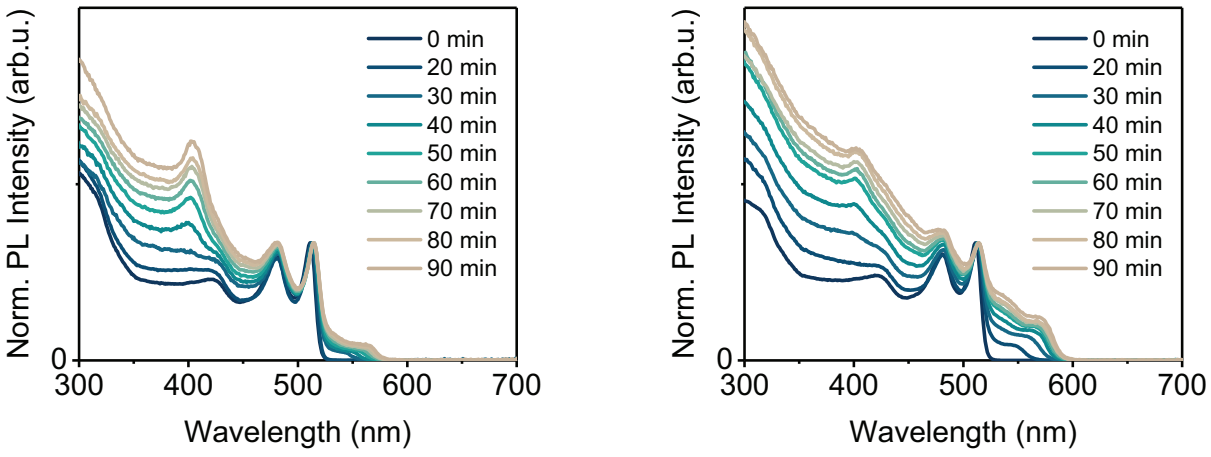

Figure S13. PL excitation spectra of CdSe/CdS core/crown NPLs synthesised from quasi-quadratic core NPLs at a rate of 6 mL h^{-1} applying (a) the single or (b) the double amounts of $Cd(Ac)_2$ and OlA. All spectra were recorded at the wavelength of the bathochromically shifted peak, if possible.

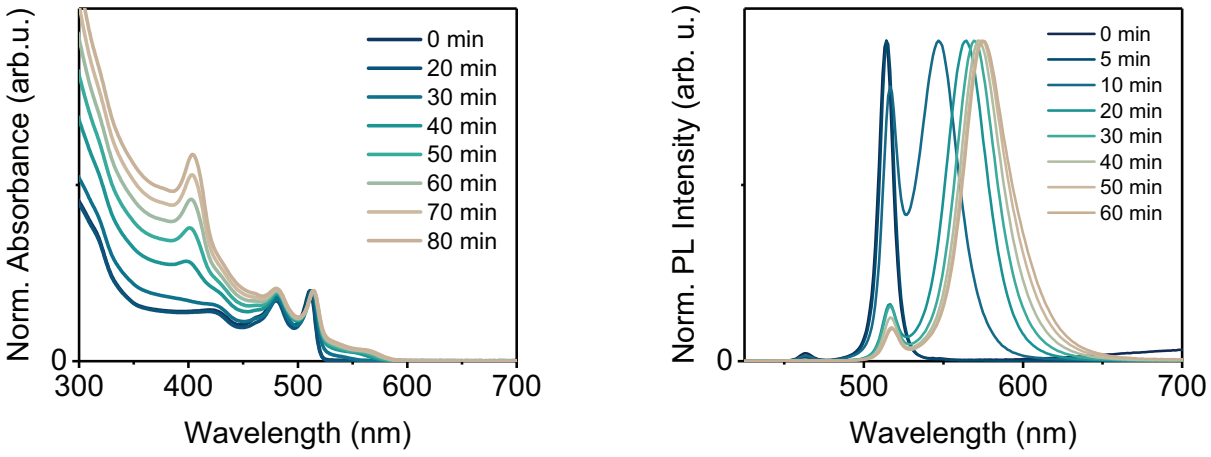

Figure S14. (a) Normalised absorbance and (b) PL emission spectra of CdSe/CdS core/crown NPLs synthesised from quasi-quadratic core NPLs at a rate of 36 mL h^{-1}. Compared to the reaction carried out at an injection rate of 6 mL h^{-1}, the formation of a thicker crown is visible at earlier reaction stages.

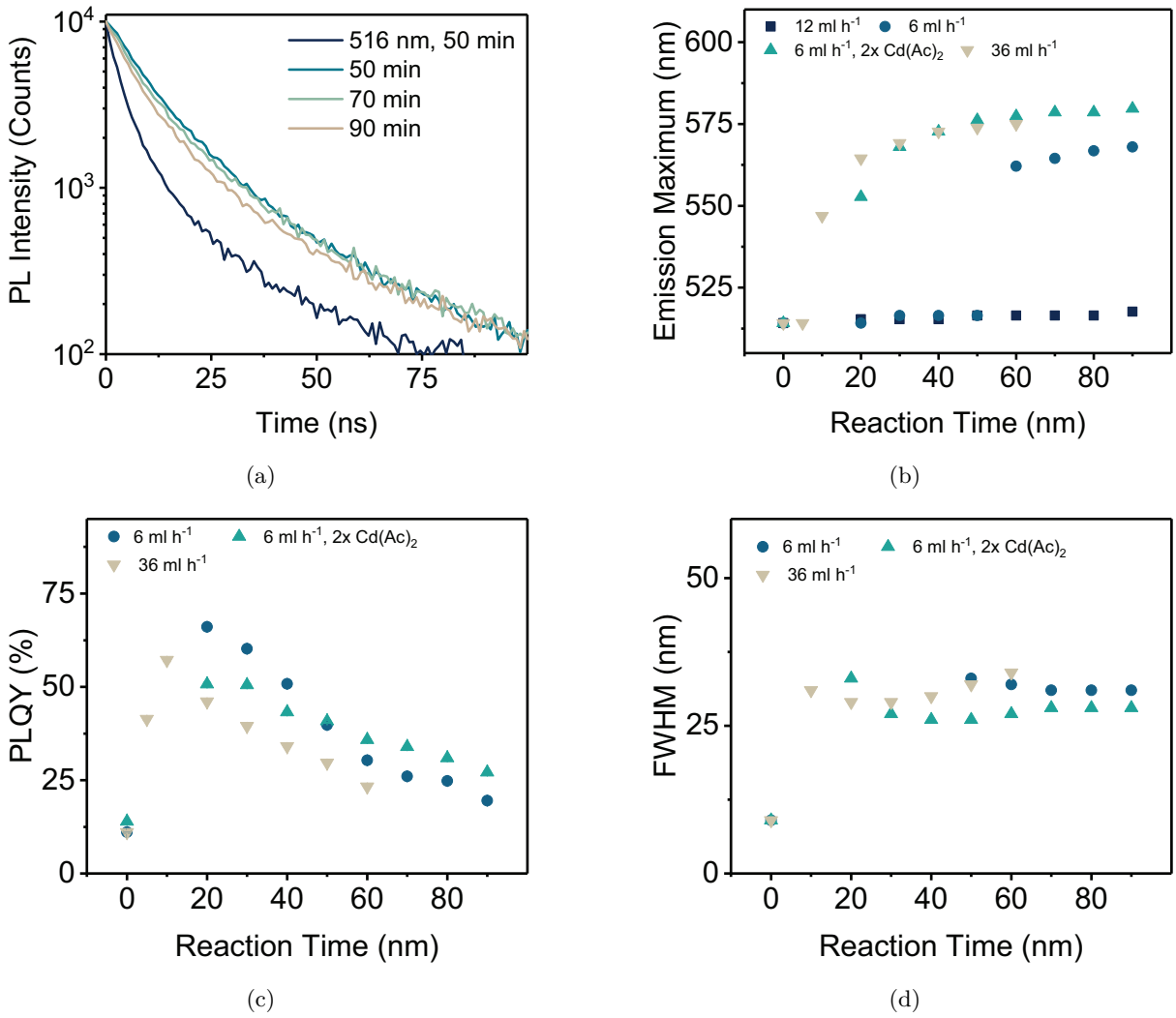

Figure S15. (a) PL decay curves of CdSe/CdS core/crown NPLs synthesised from quasi-quadratic core NPLs at a rate of 6 mL h^{-1}. For the first sample taken after 50 min reaction time, the decays were recorded at 516 nm (dark blue) and 559 nm (cyan). The decays after 70 min and 90 min were recorded at the maximum of the bathochromically shifted emission peak. The PL lifetimes obtained by fitting the decays are collected in Table S2. (b) Development of the emission maximum under different reaction conditions. (c) Development of the PLQY under different reaction conditions. All samples were excited at 400 nm. In all cases, the whole emission peak was integrated to obtain the averaged PLQY of all emitting species. (d) Development of the full width at half maximum (FWHM) of the emission peak (only bathochromically shifted emission peak) under different reaction conditions.

Table S2. Shorter and longer components and respective amplitudes of the PL decays shown in Figure S15 (a) obtained from biexponential fits

sample	emission wavelength (nm)	A_1/%	τ_1 (ns)	A_2/%	τ_2 (ns)
50 min	516	83.9	3.52	16.1	23.88
50 min	558	85.1	10.10	14.9	39.89
70 min	564	81.6	8.68	18.4	37.14
90 min	568	81.8	7.51	18.2	35.21

5 Results of powder X-ray diffractometry (PXRD).

5.1 4 ML CdSe/CdS core/crown NPLs with small quasi-quadratic cores.

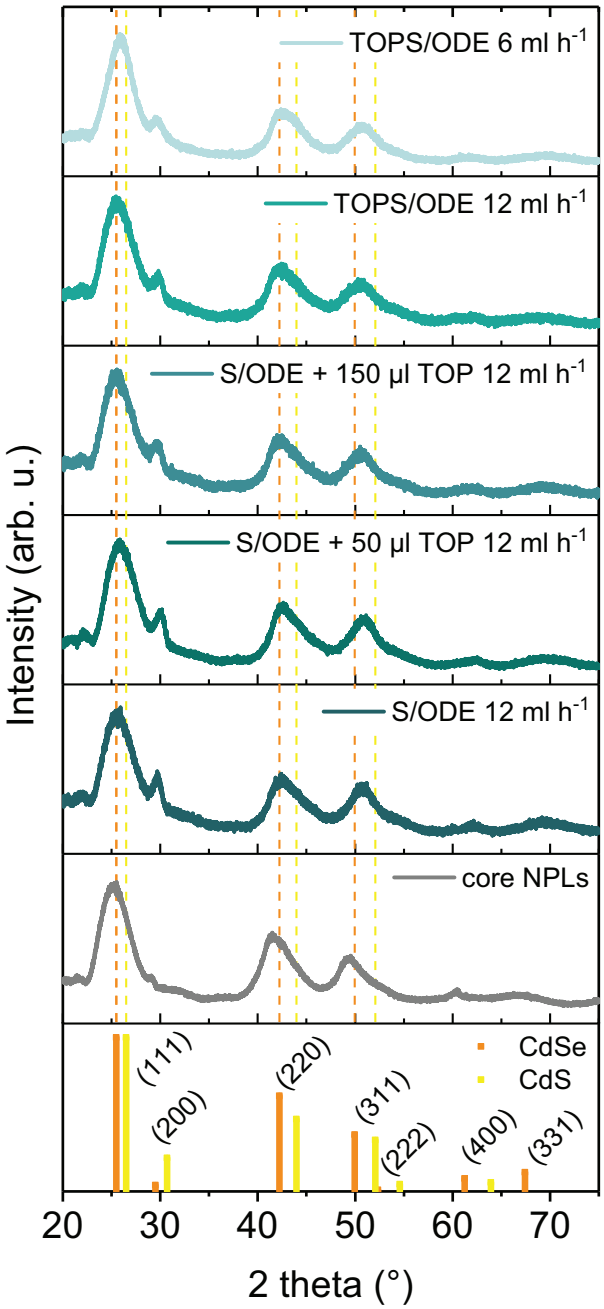

Figure S16. PXRDs of quasi-quadratic CdSe core NPLs (grey) and CdSe/CdS NPLs synthesised from quasi-quadratic cores (blue shades). In addition, the reflection positions and intensities of bulk CdSe (orange, PDF 03-065-2891) and CdS (yellow, PDF 01-075-1546) with zinc blende (ZB) structure are shown. The PXRDs of the core/crown NPLs confirm, that the ZB structure is retained during the crown growth, even if a thicker CdS crown is formed as in case of TOP/ODE 6 mL h^{-1}. In comparison to the bulk reflection positions, all reflections of the NPLs are shifted to smaller angles due to slight expansion of the lattice. The crown growth is confirmed by a shift of all reflections to higher angles (compared to the core NPL PXRD). The reflection positions and FWHM values of the (111) and (311) reflections are collected in Table S3.

Table S3. Reflection positions and FWHM values of the (111) and (311) reflections of quasi-quadratic CdSe core NPLs and CdSe/CdS NPLs synthesised from quasi-quadratic cores. The given values were obtained by fitting the reflections with Lorentz functions

sample	2θ (111) (°)	FWHM (111) (°)	2θ (311) (°)	FWHM (311) (°)
core NPLs	25.321	4.828	49.533	2.967
S/ODE 12 mL h^{-1}	25.690	5.468	50.733	3.339
S/ODE + 50 µL TOP 12 mL h^{-1}	25.978	6.203	50.835	3.470
S/ODE + 150 µL TOP 12 mL h^{-1}	25.623	5.238	50.539	3.971
TOPS/ODE 12 mL h^{-1}	25.705	5.657	50.472	4.913
TOPS/ODE 6 mL h^{-1}	25.892	3.866	50.684	4.051

5.2 4 ML CdSe/CdS core/crown NPLs with small quasi-rectangular cores.

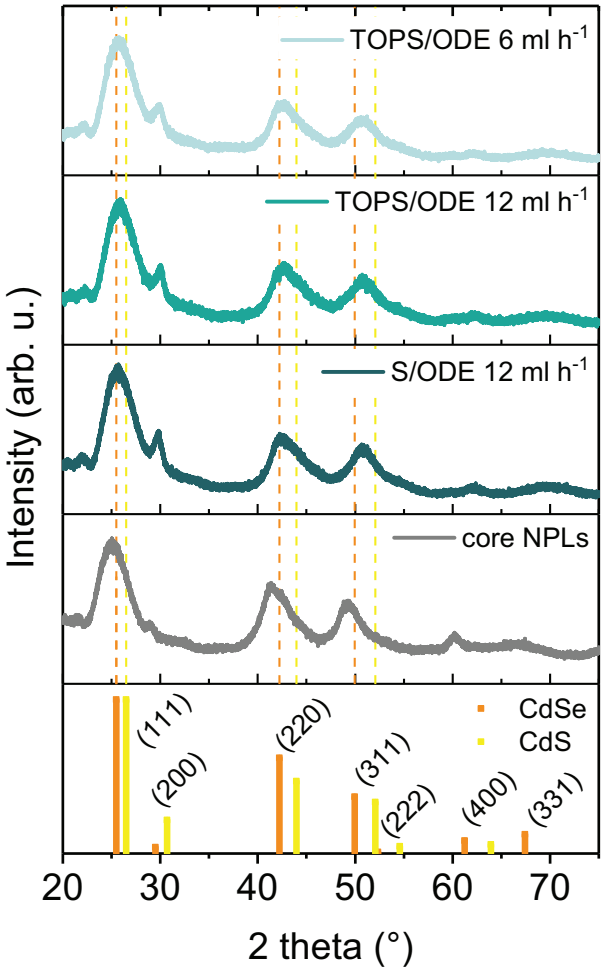

Figure S17. PXRDs of small quasi-rectangular CdSe core NPLs (grey) and CdSe/CdS NPLs synthesised from small quasi-rectangular cores (blue shades). In addition, the reflection positions and intensities of bulk CdSe (orange, PDF 03-065-2891) and CdS (yellow, PDF 01-075-1546) with zinc blende (ZB) structure are shown. In comparison to the bulk reflection positions, all reflections of the NPLs are shifted to smaller angles due to slight expansion of the lattice. The PXRDs of the core/crown NPLs confirm, that the ZB structure is retained during the crown growth. Due to the crown growth a shift of all reflections to higher angles (compared to the core NPL PXRD) is visible.

5.3 4 ML CdSe/CdS core/crown NPLs with large quasi-rectangular cores.

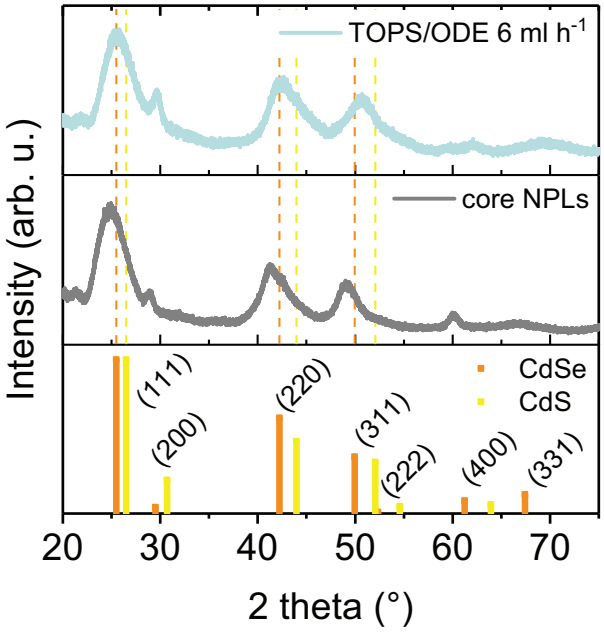

Figure S18. PXRDs of large quasi-rectangular CdSe core NPLs (grey) and CdSe/CdS NPLs synthesised from large quasi-rectangular cores (light blue). In addition, the reflection positions and intensities of bulk CdSe (orange, PDF 03-065-2891) and CdS (yellow, PDF 01-075-1546) with zinc blende (ZB) structure are shown. In comparison to the bulk reflection positions, all reflections of the NPLs are shifted to smaller angles due to slight expansion of the lattice. The PXRD of the core/crown NPLs confirms, that the ZB structure is retained during the crown growth. Due to the crown growth a shift of all reflections to higher angles (compared to the core NPL PXRD) is visible.

5.4 5 ML CdSe/CdS core/crown NPLs with large quasi-rectangular cores.

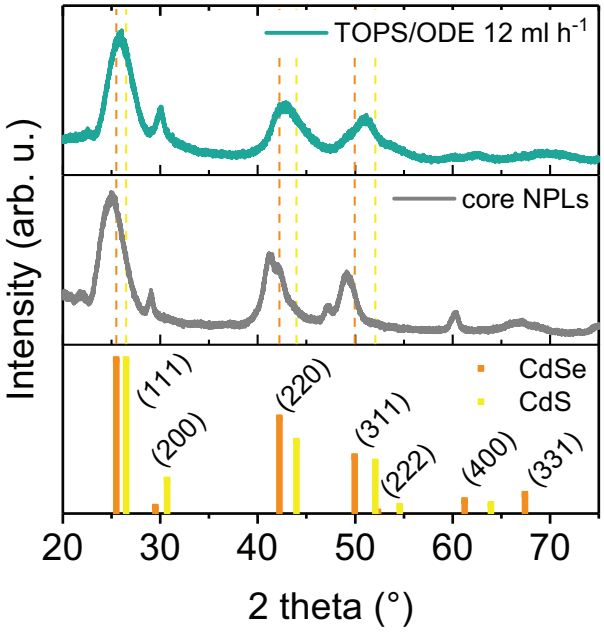

Figure S19. PXRDs of large quasi-rectangular 5 ML CdSe core NPLs (grey) and 5 ML CdSe/CdS NPLs synthesised from large quasi-rectangular cores (cyan). In addition, the reflection positions and intensities of bulk CdSe (orange, PDF 03-065-2891) and CdS (yellow, PDF 01-075-1546) with zinc blende (ZB) structure are shown. In comparison to the bulk reflection positions, all reflections of the NPLs are shifted to smaller angles due to slight expansion of the lattice. In contrast to the PXRDs of 4 ML core NPLs, also a splitting of the (311) reflection can be observed. The PXRD of the core/crown NPLs confirms, that the ZB structure is retained during the crown growth. Due to the crown growth a shift of all reflections to higher angles (compared to the core NPL PXRD) is visible.

6 TEM characterisation of 4 ML CdSe/CdS NPLs synthesised from small quasi-rectangular CdSe NPLs.

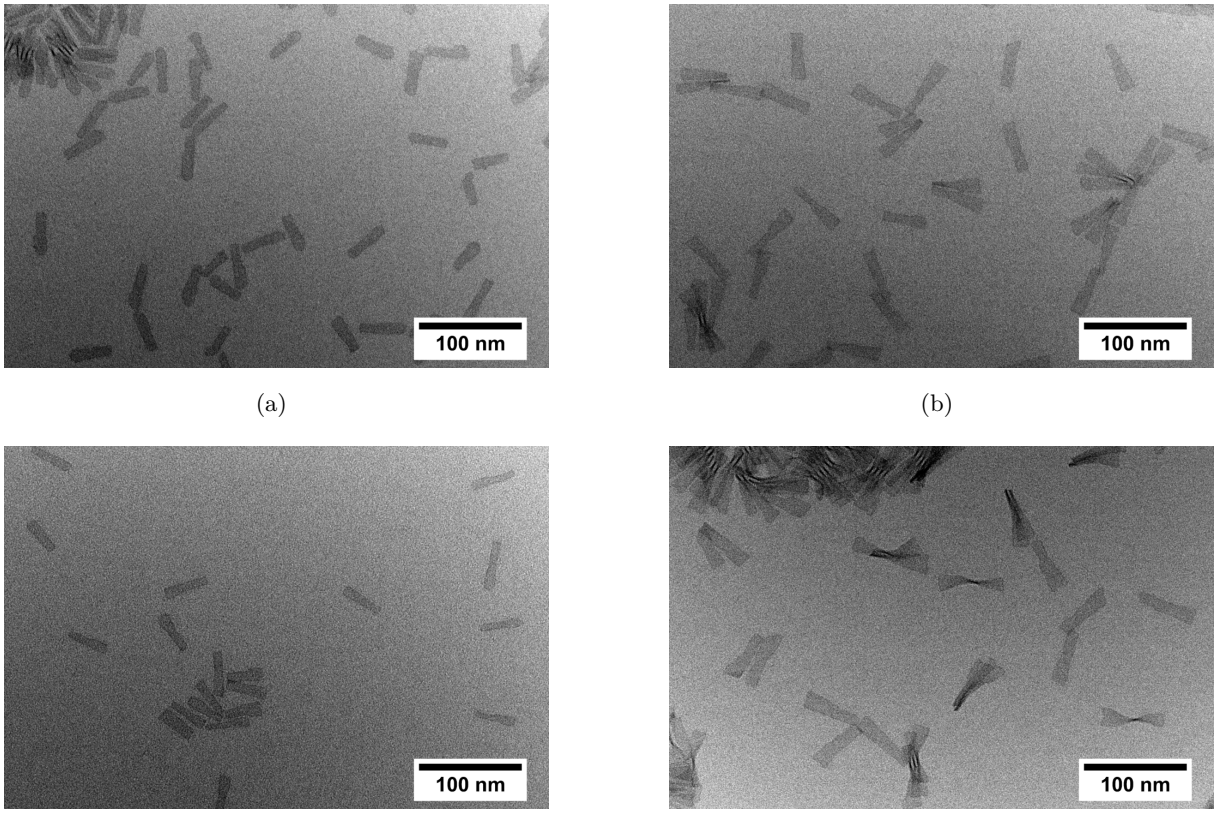

(a) (b)

(c) (d)

Figure S20. TEM images of CdSe/CdS NPLs synthesised from small quasi-rectangular core NPLs. Reaction conditions: injection rate of (a) 12 mL h^{-1} or (b)-(d) 6 mL h^{-1}, 6 mL of TOPS/ODE precursor. (a)+(b) The samples were taken when 5 mL of the precursor solution were injected [corresponding to (a) 25 min and (b) 50 min reaction time]. (c) Sample was taken after 30 min reaction time. (d) Sample was taken after 70 min reaction time. In (a)+(c), the NPL corners on one of the shorter edge are slightly rounded, as it was also observed for core/crown NPLs synthesised from larger quasi-rectangular 4 ML cores [Figure 5 (a) top].

7 Further optical characterisation of CdSe/CdS NPLs synthesised from quasi-rectangular 4 and 5 ML CdSe NPLs.

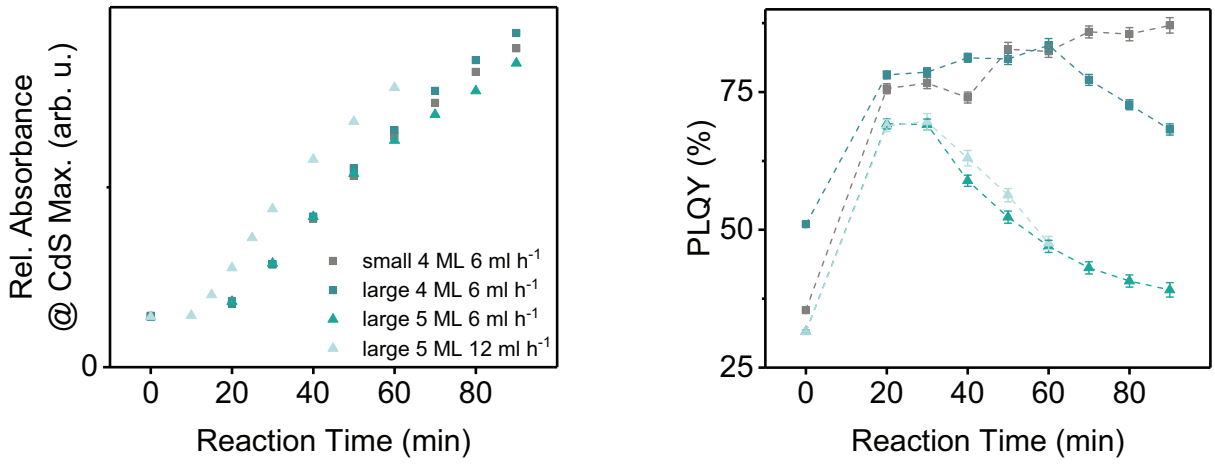

(a) (b)

Figure S21. (a) Progress of CdS crown growth on quasi-rectangular CdSe cores with different geometries and thicknesses. In all cases, 6 mL of a TOPS/ODE precursor solution were injected. It can be seen, that the growth rate is nearly independent from the applied CdSe core (for the same injection rate of 6 mL h^{-1}). However, due to the different sizes of the core NPLs, the absolute area of the CdS crown increases with increasing core size (Rel. Absorbance is directly proportional to A_{CdS}/A_{CdS}). (b) Development of the PLQY during the crown growth reactions shown in (a). Excitation wavelengths: 460 nm for 4 ML NPLs, 500 nm for 5 ML NPLs (in order to avoid excitation of the CdS crown in both cases). For small quasi-rectangular 4 ML NPLs, the PLQY was found to increase over the whole course of the reaction. If large quasi-rectangular 4 ML NPLs served as core NPLs, a maximum of the PLQY was observed at the end of the precursor injection period. For large quasi-rectangular 5 ML NPLs, a PLQY maximum is visible at an even earlier point in the reaction. It was moreover observed, that a higher injection rate enhances the PLQY of 5 ML CdSe/CdS NPLs (at similar crown sizes).

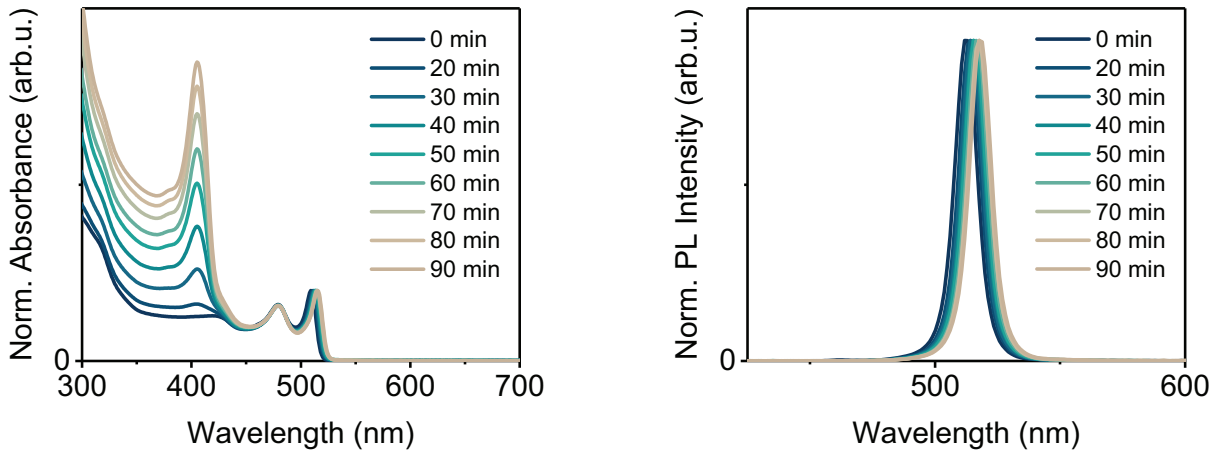

(a) (b)

Figure S22. (a) Normalised absorbance and (b) PL emission spectra of CdSe/CdS core/crown NPLs synthesised from large 4 ML quasi-rectangular core NPLs at a rate of 6 mL h^{-1}.

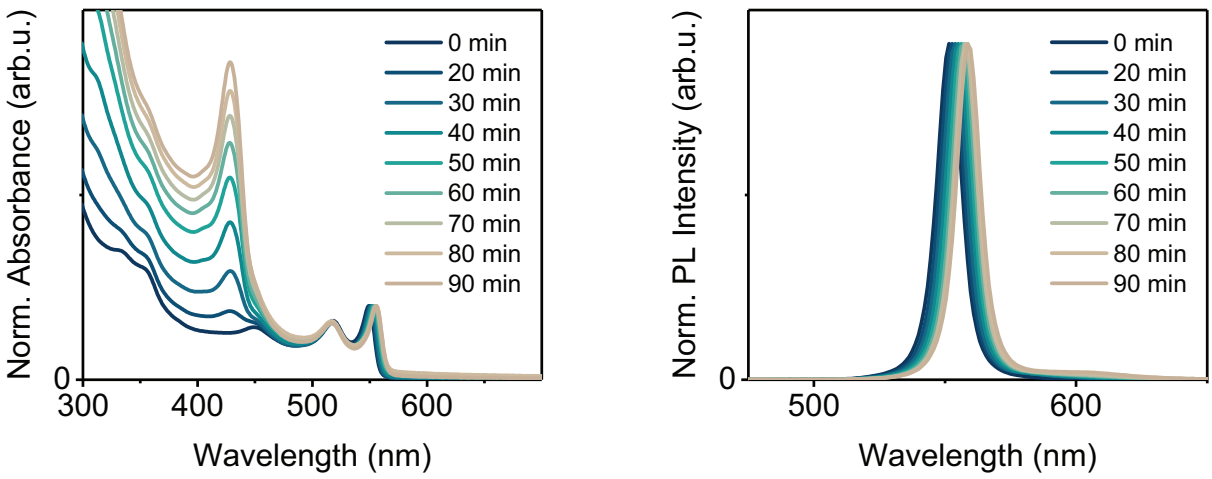

(a) (b)

Figure S23. (a) Normalised absorbance and (b) PL emission spectra of CdSe/CdS core/crown NPLs synthesised from large 5 ML quasi-rectangular core NPLs at a rate of $6\,\mathrm{mL\,h^{-1}}$.

8 Up-scaling of the synthesis procedure.

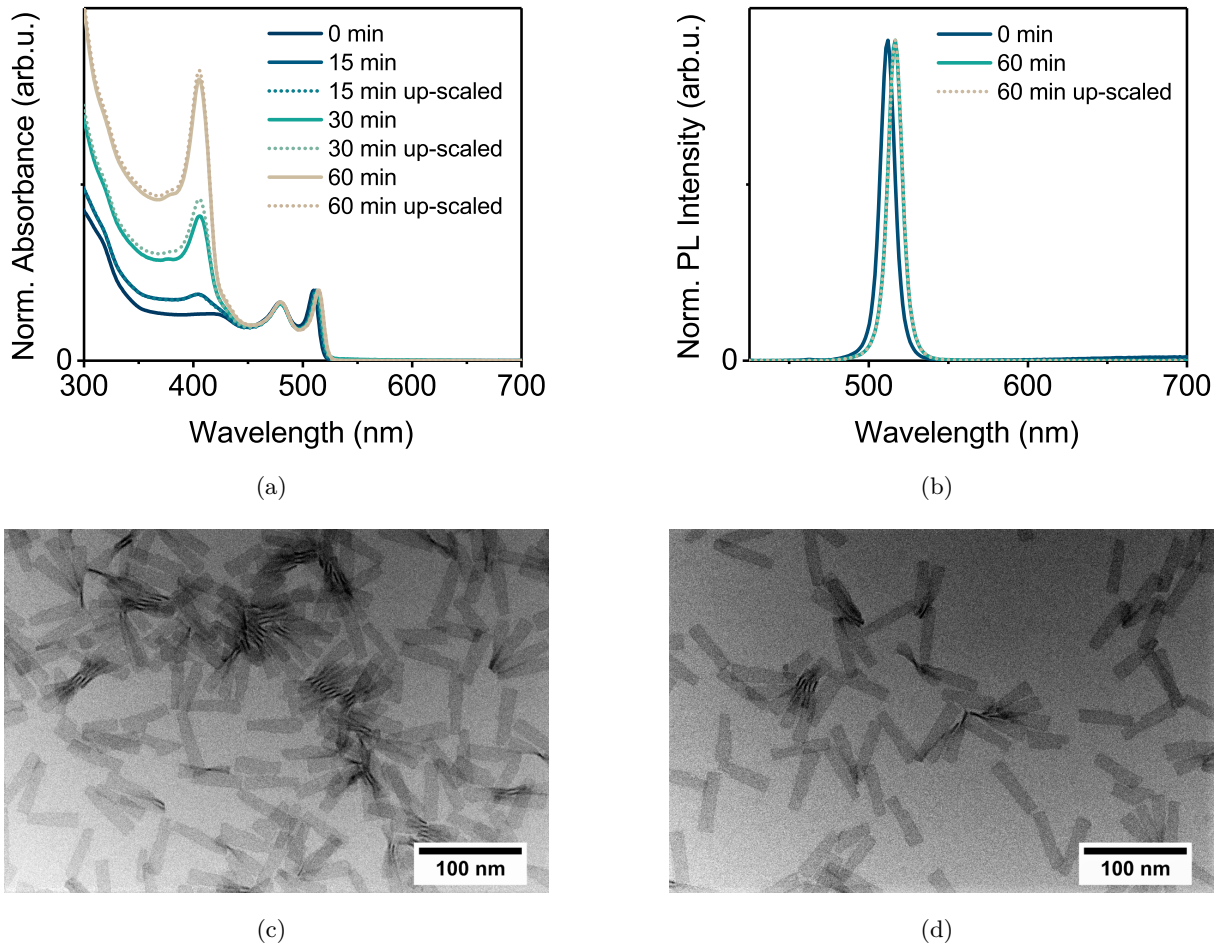

Figure S24. Characterisation results of CdSe/CdS core crown NPLs synthesised as described in the experimental section and at a five times larger scale ('up-scaled'). For both syntheses, the same batch of small quasi-rectangular 4 ML NPLs was applied. Details on the amount of reactants used are given in Table S4. (a) Absorbance spectra at different stages of the CdS crown growth. Only slight differences in the growth speed are observed. (b) PL emission spectra of the core NPLs (dark blue) and the CdSe/CdS core/crown NPLs synthesised at different reaction scales. (c)+(d) TEM images of the final CdSe/CdS core/crown NPLs synthesised (c) at a 'normal' scale and (d) at a five times larger scale. PLQYs of 86.8 ± 1.2 % and 80.1 ± 1.1 % were determined for the NPLs shown in (c) and (d), respectively.

Table S4. Reaction parameters and reactant amounts applied in the up-scaled synthesis.

reactant/synthesis parameter	'normal' scale	5 times up-scaled
V(CdSe NPLs)/µL	658	3290
c_{Cd}(CdSe NPLs)/mM	70.82	70.82
m[$Cd(Ac)_2$]/mg	96	480
V(ODE)/mL	8	40
V(OlA)/mL	180	900
V(TOPS, 1 M)/µL	300	1500
V(ODE)/mL	5.7	13.5
injection rate/mL/h	12	30

9 Comparison to CdSe and CdTe crown growth.

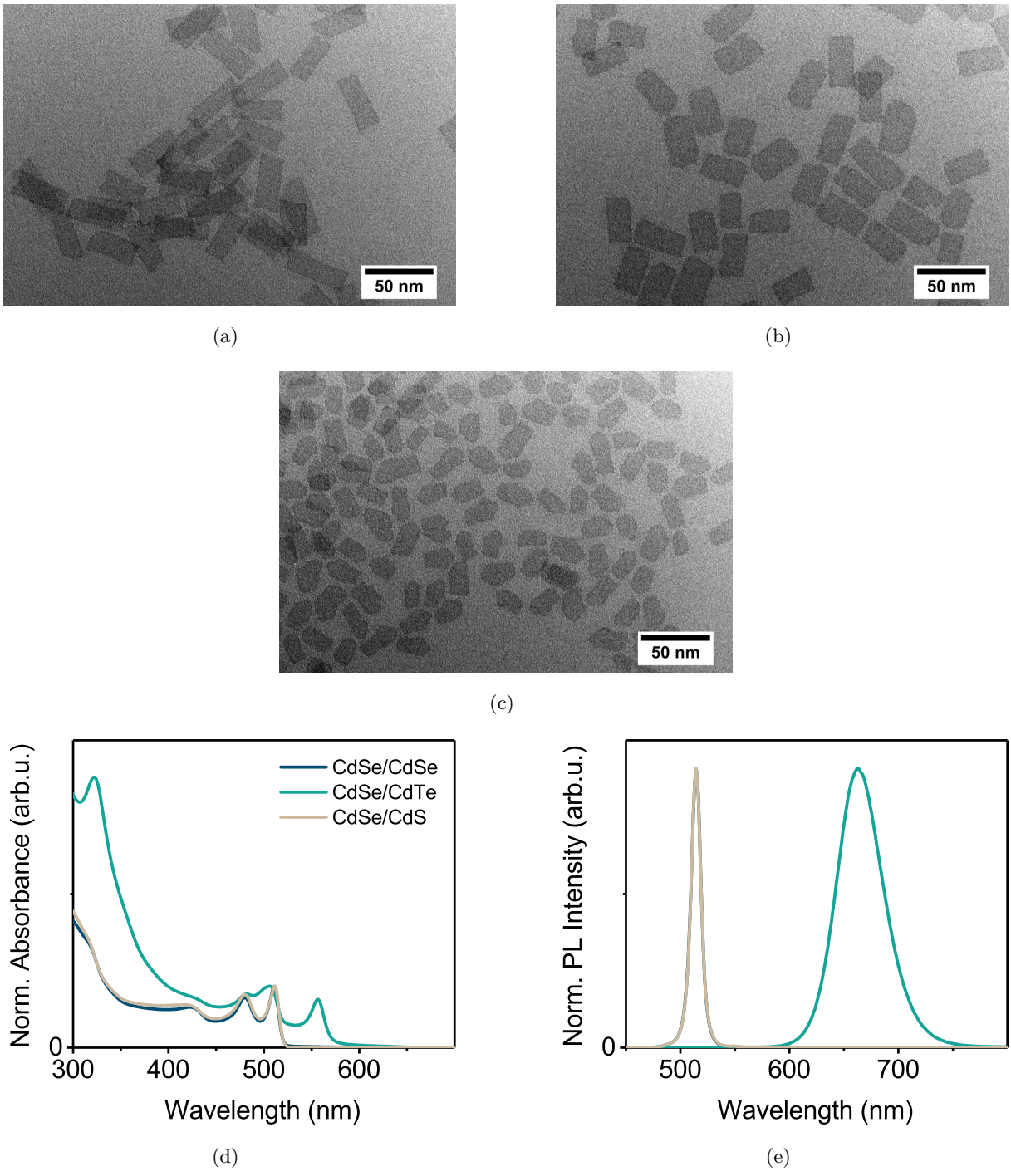

(a) (b) (c) (d) (e)

Figure S25. (a)-(c) TEM images of (a) CdSe/CdSe, (b) CdSe/CdTe and (c) CdSe/CdS core/crown NPLs synthesised from quasi-quadratic core NPLs. (d) Absorbance spectra and (e) PL emission spectra of the respective core/crown NPLs. In all cases, 2 mL of a 50 mM precursor solution were injected at 6 mL h^{-1}. For CdSe and CdTe growth TOPSe/ODE and TOPTe/ODE were injected, respectively, for CdS growth S/ODE was used. In the TEM images it can be seen, that the CdSe and CdTe crown growth proceed much faster than the CdS growth even if TOP containing precursors are applied. This is in part caused by the much higher reactivities of TOPTe and TOPSe in comparison to TOPS (and S/ODE).[2] In spite of their fast crown growth process, the CdSe/CdSe and CdSe/CdTe core/crown NPLs are still characterised by a very uniform size and shape with well-defined edges and corners. This implies, that the crown growth rates vary strongly for the different edge facets in case of CdSe and CdTe growth, whereas they are rather similar (and much lower) in case of CdS growth.

References

[1] S. Ithurria, M. D. Tessier, B. Mahler, R. P. S. M. Lobo, B. Dubertret and A. L. Efros, *Nature Materials*, 2011, **10**, 936–941.

[2] L. A. Swafford, L. A. Weigand, M. J. Bowers, J. R. McBride, J. L. Rapaport, T. L. Watt, S. K. Dixit, L. C. Feldman and S. J. Rosenthal, *Journal of the American Chemical Society*, 2006, **128**, 12299–12306.